energies

MDPI

Article

Investigation of the Physico-Chemical Properties of the Products Obtained after Mixed Organic-Inorganic Leaching of Spent Li-Ion Batteries

Weronika Urbańska [1,*] and Magdalena Osial [2]

[1] Department of Environmental Engineering, Wrocław University of Science and Technology, Wybrzeże Wyspiańskiego 27, 50-370 Wrocław, Poland
[2] Faculty of Chemistry, University of Warsaw, Pasteura 1 Street, 02-093 Warsaw, Poland; mosial@chem.uw.edu.pl
* Correspondence: weronika.urbanska@pwr.edu.pl

Received: 9 November 2020; Accepted: 17 December 2020; Published: 20 December 2020

Abstract: Lithium-ion batteries are currently one of the most important mobile energy storage units for portable electronics such as laptops, tablets, smartphones, etc. Their widespread application leads to the generation of large amounts of waste, so their recycling plays an important role in environmental policy. In this work, the process of leaching with sulfuric acid for the recovery of metals from spent Li-ion batteries in the presence of glutaric acid and hydrogen peroxide as reducing agents is presented. Experimental results indicate that glutaric-acid application improves the leaching performance compared to the use of just hydrogen peroxide under the same conditions. Obtained samples of leaching residues after mixed inorganic-organic leaching were characterized with Scanning Electron Microscopy, Fourier Transform Infrared Spectroscopy, and X-ray diffraction.

Keywords: acid leaching; battery recycling; Li-ion batteries; metal recovery; raw material sustainable use

1. Introduction

Lithium-ion batteries and accumulators are used in a wide variety of devices—mobile phones, laptops, tablets, but also children's toys and medical equipment. In general, batteries made our life easier and revolutionized the world—thanks to the possibility of using cells as an electricity source, many devices have become mobile, making them more attractive. Complex battery packs are also used in the automotive industry—as a power source for modern hybrid or electric cars. Despite their many advantages, the widespread use of batteries has some drawbacks, mainly due to the quite complex composition of the cells. Lithium-ion batteries are made up of a graphite anode and a cathode, made out of a $Li_xMe_yO_n$ type compound—the most commonly used is lithium cobaltate, $LiCoO_2$. Lithium-ion cells also contain an organic electrolyte, which is usually lithium salts dissolved in a mixture of organic solvents (e.g., salts—$LiClO_4$, $LiPF_6$, $LiBF_4$; solvents—dimethylsulfoxide, propylene carbonate, diethyl carbonate). In addition, the electrodes are separated from each other by a synthetic separator—usually a polyolefin membrane, which enables the transfer of lithium ions while at the same time protecting against a short circuit that may occur as a result of direct contact of the anode with the cathode [1–5]. Each component of the Li-ion battery generates large amounts of waste, while the most hazardous ones are compounds containing heavy metals such as cobalt.

Several studies confirm that one of the main components, the lithium cobaltate, has a negative influence on the environment as well as on living organisms. It induces oxidative DNA damage causing mutagenic effect and inflammatory response, mainly caused by the cobalt release [6]. Many data show the role of Co(II) ions released from batteries, which causes the formation of OH-radical species by a

Fenton-like reaction, leading to chromosomal breaks and the formation of cancer cells [7,8]. Due to that effect, battery waste containing cobalt becomes dangerous for aquatic systems and humans, generating a huge need for recycling of the spent batteries. Compared to the production of new batteries, the processing of the waste batteries is a much more complicated and costly process. Nevertheless, due to the constant increase in the amount of this waste, technologies for recycling spent batteries to recover metals contained in them have been developed, and they are used in industrial practice around the world. The following processes are distinguished: mechanical separation, thermal treatment (pyrometallurgy) and acid leaching (hydrometallurgy). Due to the technological, environmental and economic benefits, the acid leaching of spent Li-ion batteries for cobalt and lithium recovery is widely studied in the literature. The commonly used leaching agents are inorganic acids, especially sulfuric, hydrochloric, phosphoric and nitric acids [9–12], and organic acids, e.g., citric, succinic, acetic and malic acids [13–16]. Cathode powder leaching processes are usually performed with the use of reducing agents, the presence of which may cause the metals contained in the battery mass to take a bivalent form (mainly Co(III) to Co(II)), soluble in acid solutions [17]. Most often, hydrogen peroxide is used for this purpose [18–22]. However, in recent years, there has been an increasing interest among scientists in the search for organic reducing agents, e.g., ascorbic acid [23–25]. This trend is triggered by environmental concerns, and it offers more effective metal recovery from spent Li-ion batteries.

During the acid leaching of the powder obtained from spent Li-ion batteries, many chemical reactions take place between the tested material and the added reagents (leaching agents and reducing agents), resulting in the formation of various products. In the literature, there are examples of reactions occurring during the leaching of battery powder ($LiCoO_2$ cathode), where both the leaching agent and the reducing agent are inorganic compounds (e.g., H_2SO_4 and H_2O_2) [26]. The reactions taking place between the powder material and various organic acids are more complicated. Nayaka G. P. et al. investigated the leaching process with iminodiacetic and maleic acids with the addition of ascorbic acid [24]. The authors paid attention to the formation of products in the form of lithium and cobalt complexes (the initially colorless solution turns pink over time, which indicates the transition of Co^{3+} to complex forms; lithium complexes are not colored), as well as the reducing effect of ascorbic acid on cobalt ions—a reduction from Co^{3+} to Co^{2+} (in the case of using only iminodiacetic acid in the leaching solution, two forms of cobalt were present: Co^{3+} and Co^{2+}, while for maleic acid alone, only unreduced cobalt was found—Co^{3+}). Nayaka G. P. et al. similarly presented the changes taking place during the processes, the results of which have been presented in their publications on similar topics (leaching experiments: citric acid with ascorbic acid, tartaric acid with ascorbic acid, adipic acid/nitryldiacetic acid) [25,27,28]. However, no specific record of the course of these reactions has been proposed due to the need to study the structures and chemical composition of powders after leaching each time in order to determine the compounds present in the material and their forms.

This article is focused on the determination of the chemical composition and form of compounds present in battery powders after leaching in the presence of 1.5 M H_2SO_4 as a leaching agent with or without reducing agents: 30% solution of H_2O_2 and/or $C_5H_8O_4$ (glutaric acid). The rates of metal recovery obtained as a result of acidic reductive leaching and the effects of quantitative and qualitative analysis performed with the use of the following methods: ICP-OES, SEM-EDS, FT-IR and XRD are presented and discussed.

2. Materials and Methods

In this study, various types of Li-ion batteries were used. They were obtained from numerous sources of commercial origins. They were dedicated for laptops from different manufacturers, such as Lenovo, Toshiba or Hewlett-Packard. Initially, upstream material was dismantled with the manual procedure described widely in literature, including removal of both steel and plastic cases that cover the batteries [29–31]. Anode and cathode were crushed carefully and sieved to separate particular elements such as plastic film, scrap paper, outer metallic body and membrane. Obtained battery powder was collected and used for further research. The obtained mass was subjected to XRD and SEM

analyses as well as a mineralization method. To mineralize, 0.5 g of the tested waste battery powder was spread wet in an open system using the DigiPREP Jr. mineralization system (parameters: 10.00 mL 65% HNO_3, digestion time: 5 h, temperature: 120 °C). The obtained solution was evaporated to a volume of approximately 0.5 mL, transferred quantitatively to a plastic container and supplemented with deionized water to 50 g. At the same time, a blank sample was prepared and included in the final results. The analyses were performed in parallel in three repetitions. Then the metal concentrations in the solution were determined using ICP-OES (Agilent 720).

The separated powder from spent Li-ion batteries was subjected to the leaching. Acid leaching was performed in 1.5 M sulfuric acid (96% analytical grade, STANLAB), as the reducing agents glutaric acid $C_5H_8O_4$ (5% *w*/*v*) and hydrogen peroxide H_2O_2 (30% analytical grade, STANLAB; 0.9% *v*/*v*) were used. An experiment without the addition of reducing agents was also performed in order to compare its results with samples 1, 2 and 3, and to determine the effect of reducers on the obtained recovery degrees of the tested metals. The ratio of the solid phase to the liquid phase was 1/10 in each case. Other assumed leaching parameters were: temperature—90°C, time—2 h and mixing speed—500 rpm (Table 1). The methodology of these experiments has also been demonstrated in previous studies where the results of leaching research were compared with different process parameters [32].

Table 1. Summary of the best operational conditions for leaching the battery powder.

Sample	Volume of 1.5 M H_2SO_4	Concentration of Reducing Agent	Time (h)	Slurry Density (*w*/*v*)	Temp. (°C)	Rotation Rate (rpm)
Sample 1	100 mL	0.9% H_2O_2 (*v*/*v*)	2	10/100	90	500
Sample 2	100 mL	5% $C_5H_8O_4$ (*w*/*v*)	2	10/100	90	500
Sample 3	100 mL	0.9% H_2O_2 (*v*/*v*) + 5% $C_5H_8O_4$ (*w*/*v*)	2	10/100	90	500
Sample 4	100 mL	-	2	10/100	90	500

After leaching was complete, the samples were vacuum-filtered. The content of metals Al, Ca, Co, Cr, Cu, Fe, Li, Mn, Na, Ni, Si and Zn in the leachates was determined (ICP-OES, Agilent 720) and their percent recovery degrees were determined in relation to the initial concentrations in the tested material. The samples of battery powder after leaching with reducing agents (no. 1, 2 and 3) were dried at 105 °C for 24 h in order to characterize the metal content. Then, the dried material was analyzed with microscopic and spectroscopic techniques. To determine the morphology of powder the FE-SEM Merlin (Zeiss) equipped with a Gemini II column was used. The device worked in low kV value range (0.5–1.5 kV) and low probe current 10–20 µA. EDS was used for elemental analysis of the measured samples. Complementary to the EDS analysis, for determination of the chemical composition of samples the FT-IR analysis was performed with Nicolet 8700 in range 4000-400 cm^{-1}. The powder X-ray diffraction patterns were recorded with a powder diffraction X-ray diffractometer (PXRD) X'PERT Phillips with PW 1830 generator with CuKα radiation with line λ = 1.5405980 Å and a scan rate of 0.05° per minute in 0.016° steps covering the 2θ angle range from 20° to 130°. Measurements were performed at room temperature using DHN software.

3. Results and Discussion

3.1. Mechanical Treatment

As a result of the mechanical processing of individual cells, the following fractions were obtained: ferromagnetic (metals, e.g., steel housing), diamagnetic (plastics, paper) and paramagnetic (anode and cathode—battery powder) constituting the material used for further research. The components of the entire spent cell and a single lithium-ion battery separated as a result of mechanical processing are presented in Figure 1.

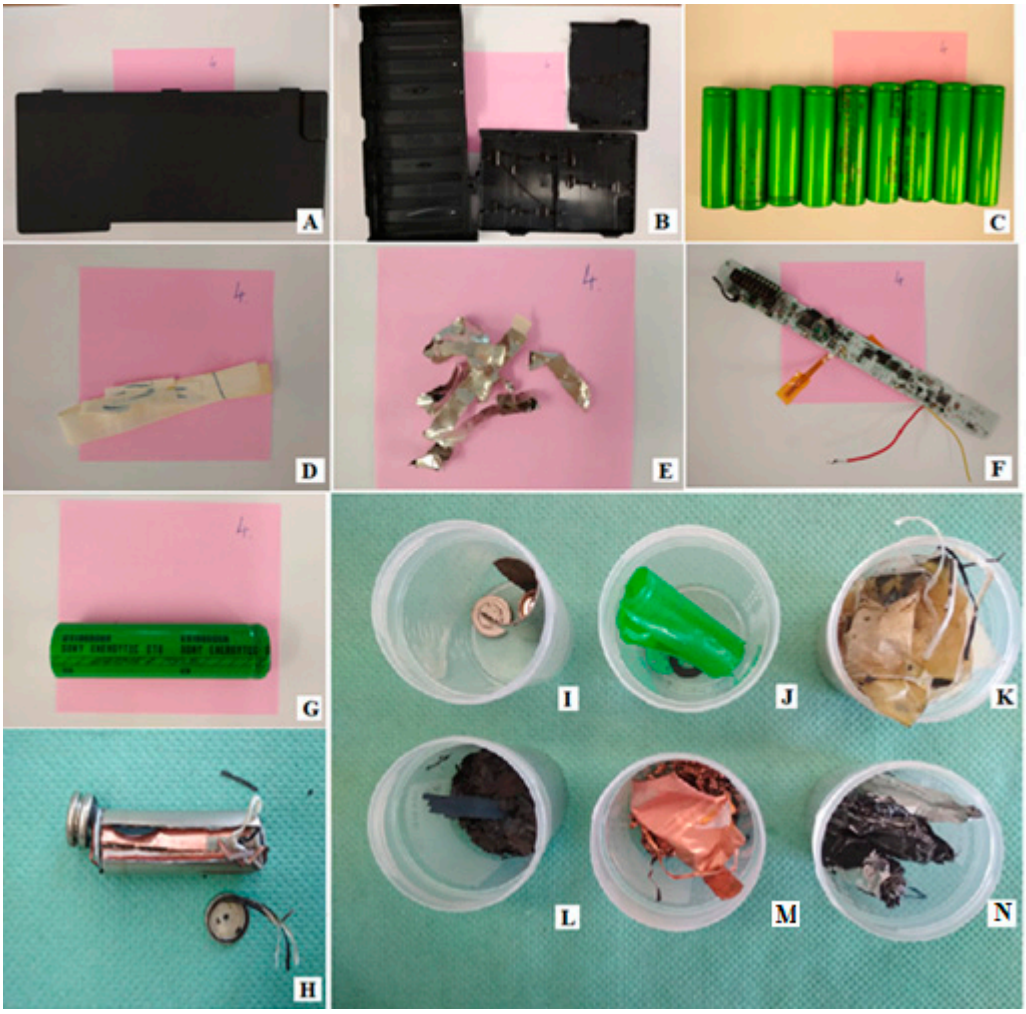

Figure 1. Mechanical treatment of a single spent lithium-ion cell. Stage I: (**A**) spent lithium-ion battery; (**B**) plastic case; (**C**) lithium-ion cells; (**D**) paper; (**E**) metals; (**F**) PCB and wires. Stage II: (**G**) single spent lithium-ion cell; (**H**) cell after cutting; (**I**) metal case; (**J**) cover and other plastics; (**K**) separator; (**L**) battery powder; (**M**) copper foil; (**N**) aluminum foil.

From the presented results, it can be concluded that the entire lithium-ion battery forms a package of individual (in this case nine) cells. Both the complete battery and a single cell are composed of many different components, such as plastics, paper or metals. The most valuable raw material is the battery mass (anode and cathode powders), rich in metals that can be successfully recovered. Battery powder constitutes more than 36% of the total mass of a single spent Li-ion cell, and it was used for further laboratory experiments. The obtained results are very similar to those in the literature [33].

3.2. *Quantitative and Qualitative Analysis of Battery Powder before Leaching*

In order to investigate the qualitative composition of the tested material, the battery powder was subjected to XRD analysis, which showed that the main components in the material are carbon and the cathode compound—$LiCoO_2$. Then the powder material was mineralized, as was the content of metal ions: Al, Ca, Co, Cr, Cu, Fe, Li, Mn, Na, Ni, Si and Zn in the obtained solution (ICP-OES, Agilent 720). It was specified that the tested battery powder contains all the marked metals, mostly cobalt, lithium and nickel (Table 2).

Table 2. Metal content in the sample of powder from the spent Li-ion batteries [32].

Metal	Al	Ca	Co	Cr	Cu	Fe	Li	Mn	Ni	Si	Zn
C (g/kg)	0.93	0.40	256.0	0.005	3.59	0.27	33.20	0.560	14.40	3.76	0.07

3.3. Acidic Reductive Leaching

As a result of the acidic reductive leaching of the tested battery powder, multiple solutions with a similar raspberry color, but different saturation, were obtained. This could already indicate the degrees of leaching of individual metals, especially cobalt responsible for the pink color of the samples. The contents of the metals in the obtained solutions were determined and presented in the form of percent recovery degrees (Table 3).

Table 3. Degrees of metal recovery from solutions after acidic reductive leaching.

Metal		Al	Ca	Co	Cr	Cu	Fe	Li	Mn	Ni	Si	Zn
Recovery, %	**Sample 1**	71.61	48.73	1.95	67.49	83.53	87.35	84.19	56.42	80.25	71.68	87.58
	Sample 2	10.64	24.58	32.30	66.25	82.12	99.45	75.86	31.22	38.77	43.30	47.66
	Sample 3	53.66	35.98	59.37	84.60	97.36	100.00	79.81	62.39	81.75	70.25	93.93
	Sample 4	49.76	34.09	30.94	47.67	79.96	93.44	72.32	31.10	37.61	58.52	50.55

Based on the results, it can be concluded that all tested metals were leached to some extent in each of the samples (see Table 3). In the case of aluminum, the highest degree of recovery was obtained for sample 1 (reducer 30% solution of H_2O_2), i.e., 71.61%; slightly lower—53.66% for sample 3, where two reducing agents were dosed; and 49.76% for sample 4 (an experiment without reducing agents). The lowest Al recovery was noted for sample 2—10.64%. Therefore, it can be concluded that the addition of glutaric acid does not significantly improve the Al leaching effects and when used with hydrogen peroxide, it may even inhibit the action of the inorganic reducing agent. Similar relationships were also obtained for calcium (1—48.73%, 2—24.58%, 3—35.98%, 4—34.09%); and silicon (1—71.68%, 2—43.30%, 3—70.25%, 4—58.52%). Relatively high levels of lithium recovery were achieved in each of the samples. The greatest amount of lithium was leached in sample 1, where the hydrogen peroxide as a reducing agent (84.19%) was used. A slightly lower degree of recovery (79.81%) was obtained in sample 3 (reducing agents—hydrogen peroxide and glutaric acid). The lowest results were recorded in samples 2 and 4 (respectively: 75.86% and 71.21%). For the other metals, i.e., Co, Cr, Cu, Fe, Mn, Ni and Zn, the highest levels of their recovery were determined for sample 3 (H_2O_2 + $C_5H_8O_4$), which confirms the assumed synergistic action of two chemical compounds used as reducers, in the tested reaction environment. Taking into account all the received results of the analyses, it can be seen that the addition of a reducing agent to the leaching process allows for obtaining higher recovery rates for most of the metals contained in the leached waste battery powder. However, the type of reagent used as a reducing agent is important. It is also worth noting that in sample 1 a very low leaching degree of cobalt was recorded (1.95%), while the use of glutaric acid as a reducing agent in sample 2 increased the recovery degree of this metal to 32.30%. Nevertheless, literature data confirm the positive influence of the presence of hydrogen peroxide used as a reducing agent on the obtained degrees of recovery of cobalt ions (reduction of Co (III) to the more easily leached form—Co (II)) [26], which could not be reproduced in the presented laboratory studies. This may be due to differences in the initial preparation of the research material and the assumed parameters of the leaching process, especially the adopted too-low dose of hydrogen peroxide. Such an assumption was made in previously conducted research [32]. The effect of an H_2O_2 dose on the sulfuric acid leaching process was investigated, where glutaric acid was also used as a reducing agent. By increasing the dose of H_2O_2 to 15 mL, it was possible to achieve almost 90% cobalt recovery, with about 96% lithium and 91% nickel recovery.

Thus, the hypothesis, that increasing the volume of H_2O_2 contributes to higher Co recovery degrees, was confirmed [32].

As mentioned before, the battery powder contained the most cobalt, lithium and nickel in its composition. The recovery of these metals from spent Li-ion batteries is most commonly studied in the research. Comparing the obtained results for Co and Ni, it can be clearly stated that the highest levels of their recovery (59.37% and 81.75%, respectively) were obtained in sample 3 leached in the presence of two reducing agents. For lithium, the highest result was obtained for sample 1, however, it is not much higher than in sample 3. Therefore, it can be concluded that taking into account the leaching of all three metals, the process parameters for sample 3 are optimal and give the best results—high efficiency of leaching of metals such as Co, Li and Ni. Detailed considerations on this subject are included in the publication [32]. Moreover, the simultaneous use of hydrogen peroxide and glutaric acid as reducing agents also allowed obtaining the highest recovery degrees of most of the tested materials: Cr (84.60%), Cu (97.36%), Fe (100%), Mn (62.39%) and Zn (93.93%). Next, the leaching residues were investigated to determine the morphology of samples, their chemical composition and crystallinity.

3.4. Morphological Studies

The morphology of leaching residues was investigated with scanning electron microscopy (SEM). Initially, SEM analysis was performed for waste battery powder before leaching. As can be seen in Figure 2, the sample has uniform morphology that is mainly based on a granulelike structure. The sample has homogeneous morphology within the whole surface.

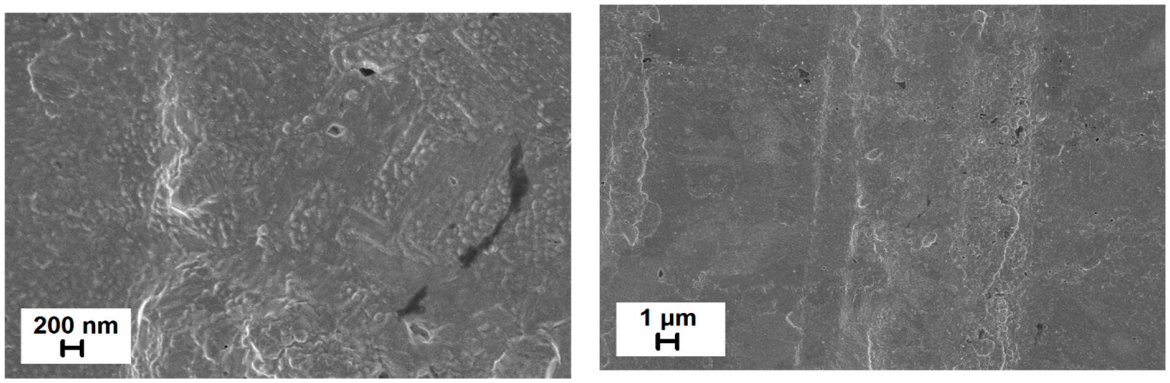

(**a**) (**b**)

Figure 2. SEM images of waste battery powder before leaching (sample 0), where (**a**) and (**b**) are presented in different scale.

Figure 3 shows images obtained for sample 1 consisting of irregular structures having a different shape and size. The morphology of the sample is similar to the whole bulk structure. As can be seen in Figure 3a, small particles having a grainlike structure about 150–200 nm are visible, however some of them tend to agglomerate, forming wirelike objects. Following images show irregular structures that seem to be crystals. They are present in the whole sample. Figure 3c reveals large objects with a round shape that tends to peel onto their surface. Based on the EDS analysis presented at Figure 3d as the map of elements the smallest granulelike objects consist mainly of cobalt or its compounds. The Following crystal-like structures consist of fluorine, while the oxygen accompanies almost all objects in the sample except the largest ones that are carbon coming from the graphite in the spent battery powder.

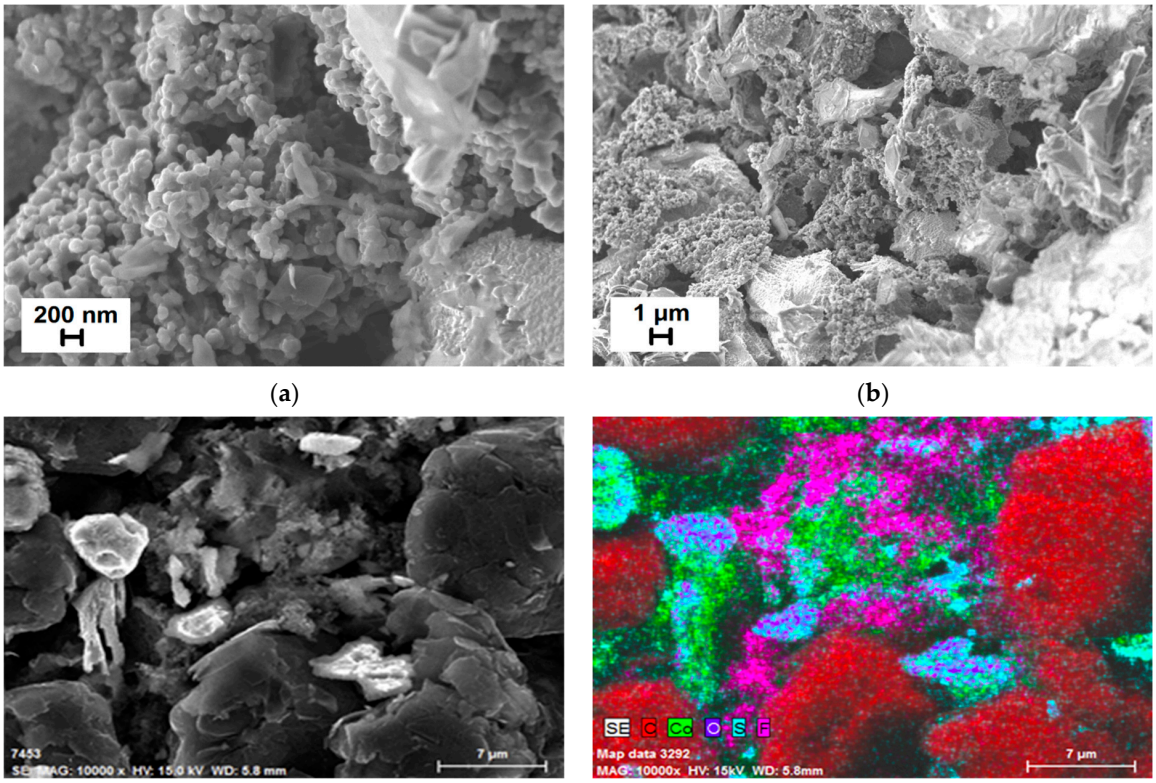

(**a**) (**b**)

(**c**) (**d**)

Figure 3. SEM images of sample 1, where (**a**–**c**) show different scales, while (**d**) is an EDS map of elements.

Following images recorded for sample 2 are presented in Figure 4. As can be seen in Figure 4a,b, this sample has a completely different shape than sample 1, and the main objects seem to be crystal-like. That sample looks more compact, and grainlike structures are not visible. Figure 4c reveals large objects that are present in the whole morphology. Their size ranges from about 1 µm up to larger than 10 µm. EDS analysis indicates that the sample is heterogeneous. Additionally, in comparison to the previous sample, it also contains manganese or its compounds that were not leaching within the procedure used for sample 2.

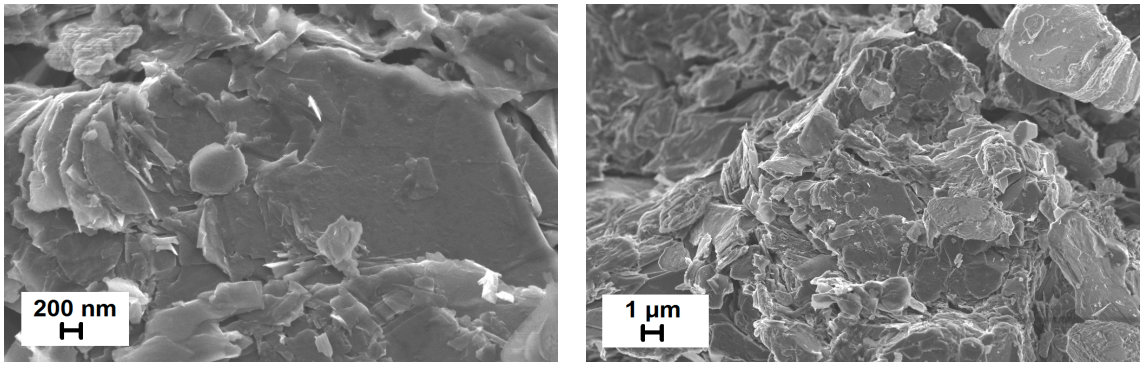

(**a**) (**b**)

Figure 4. *Cont.*

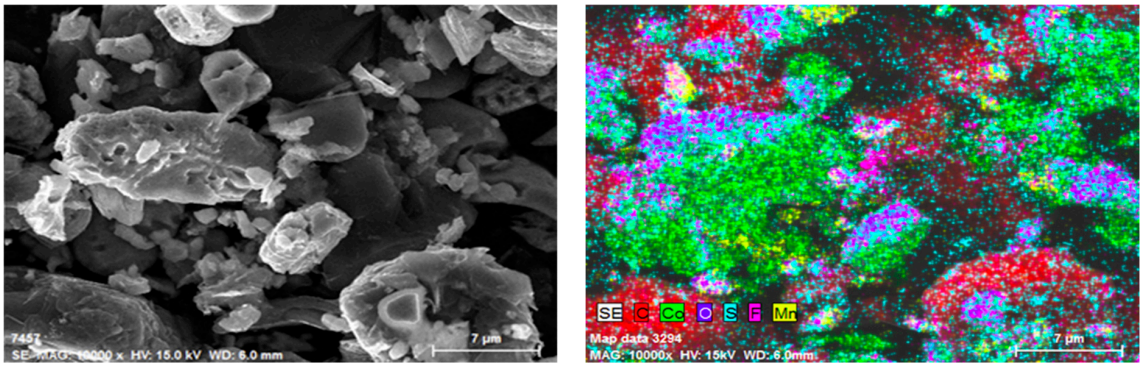

(**c**) (**d**)

Figure 4. SEM images of sample 2, where (**a**–**c**) show different scales, while (**d**) is an EDS map of elements.

The SEM images for sample 3 are presented in Figure 5. The morphology is different from samples 1 and 2. As can be seen in Figure 5a–c, the sample seems to be the most uniform, consisting of rough and compact structures. The objects present in the sample have a size from a few µm to more than 10 µm. The EDS map presented in Figure 5d reveals the elemental composition of the sample, showing large areas of carbon, looking like the substrate and objects that contain cobalt, oxygen, fluoride and even some nitrogen or their compounds. As visible, the surface of carbon is covered uniformly with sulfur that comes from the sulfuric acid during the leaching process.

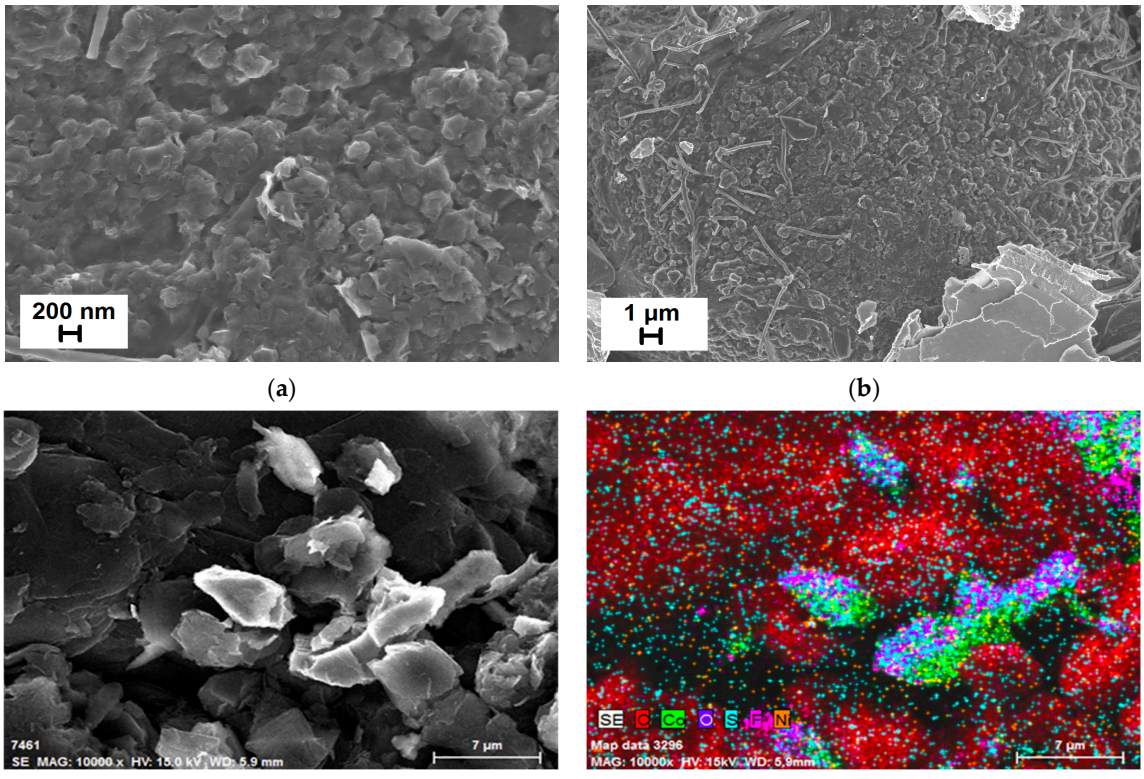

(**a**) (**b**)

(**c**) (**d**)

Figure 5. SEM images of sample 3, where (**a**–**c**) show different scales, while (**d**) is an EDS map of elements.

Meshram P. et al. [34] investigated leaching residues consisting of $LiCoO_2$, $Li_2CoMn_3O_8$ and $(Li_{0.85}Ni_{0.05})(NiO_2)$ that were leached with H_2SO_4, and revealed that the morphology of the final

product is very complex. Similarly to our results, the particles of $LiCoO_2$ are much smaller after leaching. Additionally, the final cobalt content was smaller, confirming successive recovery of that element. Lv W. et al. [35] additionally used ammonium chloride as a reducer to treat an initial sample of $Li(Ni_{0.5}Co_{0.2}Mn_{0.3})O_2$, showing that after leaching, the morphology is amorphous, and there is a lower content of Co, Ni and Mn, and a higher content of carbon. This corresponds with our experimental results. Chen X. et al. [36] treated waste battery powder consisting mainly of the $LiCoO_2$ with sulfuric acid and an organic reducer, such as glucose, saccharose and cellulose. Their research indicated that the sample of leaching residue has a more regular structure with well-defined crystallites after leaching. The efficiency of the leaching was better than without the application of organic additives. All the above-mentioned studies showed a heterogeneous product that required deep characterization with spectroscopic techniques. Therefore, to understand the chemical composition of the products obtained within this work, the FT-IR analysis was performed.

3.5. FT-IR Analysis

As shown in Figure 6, the FT-IR was employed to characterize the possible chemical composition of the obtained leaching residues. Spectra were recorded in the range of wavenumber from 4000 cm^{-1} to 400 cm^{-1} with a resolution of 5 cm^{-1}. Pure KBr pellets were used as reference material. Spectra were recorded for all three samples.

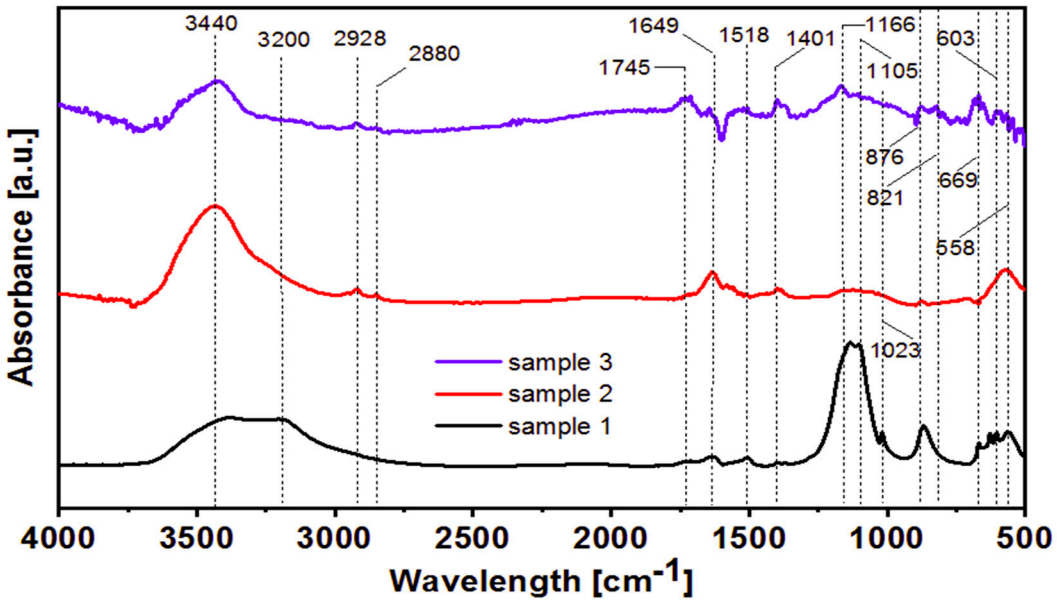

Figure 6. FT-IR spectra of battery waste powder for sample 1 that was leached with H_2SO_4 and H_2O_2, sample 2 that was leached with H_2SO_4 and $C_5H_8O_4$, and sample 3 that was leached with H_2SO_4, $C_5H_8O_4$ and H_2O_2.

The broad bands located around 3440 cm^{-1}, 3200 cm^{-1} are characteristic for vibrations of -OH group, which is absorbed onto the surface of the sample and originates from water. The band that can be ascribed to δH_2O is visible at 1649 cm^{-1} [37,38]. The two bands at 2928 cm^{-1} and 2880 cm^{-1} are characteristic for CH_2 and CH_3, respectively [39,40]. The band at 1649 cm^{-1} can be assigned to C=O stretching vibration [39], while 1745 cm^{-1} can be ascribed to stretching of -COOH [41]. Two bands at 1518 cm^{-1} and 1401 cm^{-1} may correspond to the asymmetric and symmetric vibrations of the $-COO^-$ [42,43]. The band located at 1166 cm^{-1} confirms the presence of asymmetric stretch of S=O in $-SO_3H$ groups. This comes from the leaching process with sulfuric acid. The 1105 cm^{-1} band corresponds to symmetric stretch [44,45]. The band at 1023 cm^{-1} is characteristic of the C-O vibration [46,47]. Two small bands located at 876 cm^{-1} and 821 cm^{-1} can be attributed to -C-H vibration.

Following bands at 669 cm^{-1} and 558 cm^{-1} can be assigned to νCo-O vibrations that confirm the formation of Co_2O_2 nanocrystals [48–50]. The band at 603 cm^{-1} is unclear, and it can be ascribed to Co-O stretching or -OH vibration from the water molecule [50,51].

As can be seen in Figure 6, the spectrum recorded for sample 1 (black curve) that was leached with H_2SO_4 and H_2O_2 reveals strong bands at 1166 cm^{-1} and 1105 cm^{-1}. These two are the most intensive among all samples. Obtained results correspond with previous analyses that indicated the presence of sulfur or its compounds with EDS mapping and formation of Li_2SO_4 within the XRD studies. The presence of a strong band in the spectra confirms the formation of the chemical reaction of the acid with the substrate and formation of a compound with S=O groups. Following samples also have these bands, while their intensity confirms lower content of sulfur-based compounds. The bands characteristic to the carbon-based compounds have the highest intensity for sample 3, which confirms the most efficient leaching and corresponds with the above-mentioned analyses.

Based on the recorded spectra it is clear that depending on the leaching method, the chemical composition and content of species change. Procedure 2 seems to be the least efficient towards the recovery of metals, while the most efficient one is procedure 3, where both glutaric acid and hydrogen peroxide were used as reducing agents. Following measurements were performed for a deeper understanding of the chemical composition of the species formed in the samples after the leaching process.

3.6. Crystallographic Structure

The XRD patterns were recorded in the diffraction angle (2θ) range from 15° to 85°, with a scan rate of 1°/min. The diffractogram that is presented in Figure 7 shows the patterns for the sample before leaching. The observed X-ray reflecting Bragg angle positions of $LiCoO_2$ for (003) is about 19.5° [49,52]. The following pattern located at 37.3° angle can be described as (001), while the next pattern that has high intensity of about 45° is characteristic to the (104) plane.

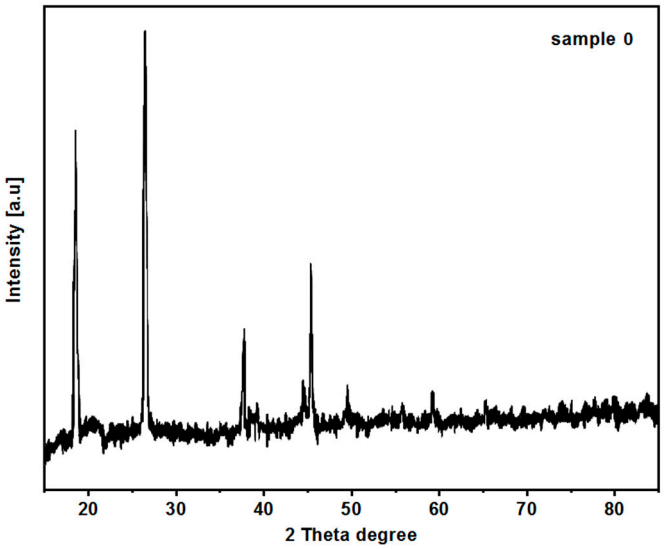

Figure 7. XRD pattern of battery waste powder before leaching (sample 0).

Figure 8 shows the reflection patterns recorded for samples after acid treatment. All samples are highly polycrystalline, and the sharp peaks confirm the formation of well-defined crystallites. The highest intensity of the reflection patterns was observed for sample 2, where the leaching agents were sulfuric and glutaric acids. The lowest intensity was observed for sample 3, where the hydrogen peroxide was used additionally. It suggests that without hydrogen peroxide the leaching process is less effective than with it.

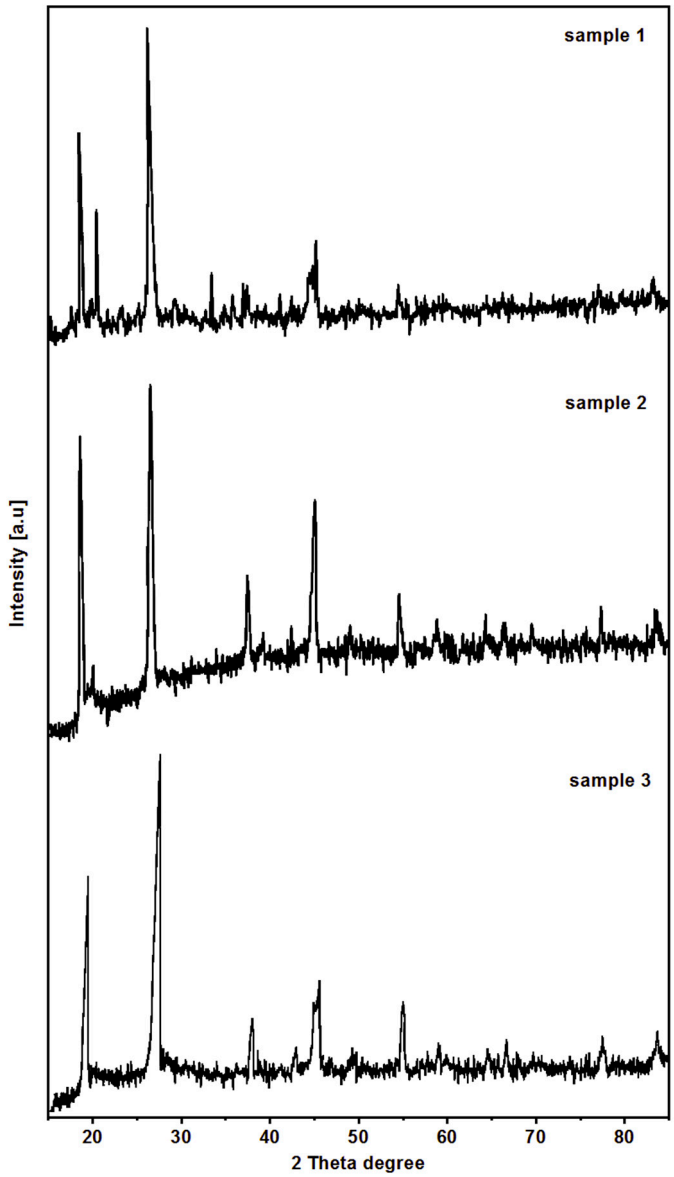

Figure 8. XRD pattern of battery waste powder for sample 1 that was leached with H_2SO_4 and H_2O_2, sample 2 that was leached with H_2SO_4 and $C_5H_8O_4$, and sample 3 that was leached with H_2SO_4, $C_5H_8O_4$ and H_2O_2.

XRD data revealed that sample 1 presented in Figure 8 has multiple patterns with predominant peaks at the angles: 18.7°, 19.5°, 27° and about 45°. The peak located at 18.7° diffraction angle can be ascribed to Co_3O_4 (111), along with lower peaks at 37.5° corresponding to the (111), 39.1° for (222), while 45° can be attributed to the (400) plane or (104) that is characteristic to $LiCoO_2$ [53,54]. Based on the literature, this peak could be also attributed to the $CoSO_4$ [55]; however, based on the EDS analysis it can be also ascribed to the LiF [56–58]. As can be seen, the pattern that spears at all samples about 19.5° is ascribed to $LiCoO_2$ for (003) [49,52], while 37.3° angle can be described as (001), 39.1° as (102) as well as the above mentioned (222) plane for Co_3O_4. The peak around the 55° angle can be ascribed to the presence of carbon in the sample. The peak at 27° can be ascribed to the carbon [59] or formation of Li_2SO_4 under the sulfuric acid treatment, which may be also ascribed to the small peak at 42.1° [60,61].

Application of glutaric acid instead of hydrogen peroxide leads to the changes in the XRD patterns. The main difference for sample 2 is presented in Figure 8. The difference is the lack of the peak at the 19.5° angle that corresponds to the (003) $LiCoO_2$. However, other peaks have a higher intensity

than for sample 1. Additionally, the presence of the peak corresponding to the C (102) is more visible. The diffractogram also reveals a pattern for carbon at about a 77.5° angle. XRD patterns obtained for sample 3 reveal similar crystallinity to sample 2, while the intensity of reflection patterns is slightly lower.

Diffractograms confirm that the main components of all samples are $LiCoO_2$ and Co_3O_4. The results are in good agreement with JCPDS data no. 75-0532 that are indexed to the hexagonal structure $LiCoO_2$, JCPDS data no. 43-1003 for literature data [62–65].

All results of XRD analyses were normalized between 0 to 1 values. As can be seen, the peak visible at 26.6° corresponds to the carbon (JCPDS 98-061-7290). The presence of carbon comes from the graphite-base anode. The high content of $LiCoO_2$ as well as Co_3O_4 in all samples suggests that the leaching agents did not completely dissolve inorganic species in the waste battery powders.

4. Conclusions

In this paper, the influence of the leaching reagent on the metallic component recovery was investigated. Sulfuric acid was used as a leaching agent, while different reducing agents were used: sample 1—treatment with H_2SO_4 and H_2O_2, sample 2—treatment with H_2SO_4 and $C_5H_8O_4$, and sample 3—treatment with H_2SO_4, $C_5H_8O_4$ and H_2O_2. Application of the ICP-OES technique revealed that procedure 2 was the least effective towards metal recovery. In this procedure H_2O_2 was used as a reducing agent. The most effective procedure was observed for sample 3, where both hydrogen peroxide and glutaric acid were used.

The results of morphological studies by SEM and elemental analysis with EDS indicated that the samples were highly heterogeneous with large carbon content. A sample that was leached with both inorganic and organic reducer was the most regular, and the leached residue mainly had large objects that were carbon. The smaller crystallites came from an inorganic phase containing metals. Moreover, the results of FT-IR and XRD analysis revealed that the main components of the waste Li-ion battery powders and leaching residues were $LiCoO_2$, Co_3O_4 and carbon originating from the graphite in the battery. The content of $LiCoO_2$ and Co_3O_4 was the largest in the sample that was leached with use of glutaric acid and hydrogen peroxide in the same bath. Thus, this work presents a successful attempt to use glutaric acid in the presence of hydrogen peroxide towards metal recovery from spent Li-ion batteries.

Author Contributions: Conceptualization, W.U. and M.O.; methodology, W.U. and M.O.; software, W.U. and M.O.; validation, W.U. and M.O.; formal analysis, W.U. and M.O.; investigation, W.U. and M.O.; resources, W.U. and M.O.; data curation, W.U. and M.O.; writing—original draft preparation, W.U. and M.O.; writing—review and editing, W.U. and M.O.; visualization, W.U. and M.O.; supervision, W.U. and M.O.; project administration, W.U. and M.O.; funding acquisition, W.U. and M.O. All authors have read and agreed to the published version of the manuscript.

Funding: This research received no external funding.

Institutional Review Board Statement: Not applicable.

Informed Consent Statement: Not applicable.

Data Availability Statement: The data presented in this study are available on request.

Acknowledgments: The authors would like to thank Jakub Lewandowski and Karol Masztalerz for technical assistance.

Conflicts of Interest: The authors declare no conflict of interest.

References

1. Czerwiński, A. *Akumulatory, Baterie, Ogniwa*; WKŁ: Warszawa, Poland, 2018. (In Polish)
2. Moćko, W.; Szmidt, E. Recovery Technologies of Co and Li from spent lithium-ion cells. *Arch. Waste Manag. Environ. Prot.* **2012**, *14*, 1–10.
3. Scrosati, B.; Garche, J. Lithium batteries: Status, prospects and future. *J. Power Sources* **2010**, *195*, 2419–2430. [CrossRef]

4. Goodenough, J.B.; Park, K.-S. The Li-Ion Rechargeable Battery: A Perspective. *J. Am. Chem. Soc.* **2013**, *135*, 1167–1176. [CrossRef] [PubMed]
5. Tarascon, J.M.; Armand, M. Issues and challenges facing rechargeable lithium batteries. *Nature* **2001**, *414*, 359–367. [CrossRef] [PubMed]
6. Sirnoval, V.; Scagliarini, V.; Murugadoss, S.; Tomatis, M.; Yakoub, Y.; Turci, F.; Hoet, P.; Lison, D.; van den Brule, S. $LiCoO_2$ particles used in Li-ion batteries induce primary mutagenicity in lung cells via their capacity to generate hydroxyl radicals. *Part. Fibre. Toxicol.* **2020**, *17*, 6. [CrossRef] [PubMed]
7. De Boeck, M.; Lison, D.; Kirsch-Volders, M. Evaluation of the in vitro direct and indirect genotoxic effects of cobalt compounds using the alkaline comet assay. Influence of interdonor and interexperimental variability. *Carcinogenesis* **1998**, *19*, 2021–2029. [CrossRef]
8. Kang, D.H.P.; Chen, M.; Ogunseitan, O.A. Potential Environmental and Human Health Impacts of Rechargeable Lithium Batteries in Electronic Waste. *Environ. Sci. Technol.* **2013**, *47*, 10–5495. [CrossRef]
9. Lee, C.K.; Rhee, K.I. Preparation of $LiCoO_2$ from spent lithium-ion batteries. *J. Power Sources* **2002**, *109*, 17–21. [CrossRef]
10. Kang, J.; Senanayake, G.; Sohn, J.; Shin, S.M. Recovery of cobalt sulfate from spent lithium ion batteries by reductive leaching and solvent extraction with Cyanex 272. *Hydrometallurgy* **2010**, *100*, 168–171. [CrossRef]
11. Joulié, M.; Lacournet, R.; Billy, E. Hydrometallurgical process for the recovery of high value metals from spent lithium nickel cobalt aluminum oxide based lithium-ion batteries. *J. Power Sources* **2014**, *247*, 551–555. [CrossRef]
12. Zhuang, L.; Sun, C.; Zhou, T.; Li, H.; Dai, A. Recovery of valuable metals from $LiNi_{0.5}Co_{0.2}Mn_{0.3}O_2$ cathode materials of spent Li-ion batteries using mild mixed acid as leachant. *Waste Manag.* **2019**, *85*, 175–185. [CrossRef] [PubMed]
13. Golmohammadzadeh, R.; Rashchi, F.; Vahidi, E. Recovery of lithium and cobalt from spent lithium-ion batteries using organic acids: Process optimization and kinetic aspects. *Waste Manag.* **2017**, *64*, 244–254. [CrossRef]
14. Li, L.; Qu, W.; Zhang, X.; Lu, J.; Chen, R.; Wu, F.; Amine, K. Succinic acid-based leaching system: A sustainable process of recovery of valuable metals from spent Li-ion batteries. *J. Power Sources* **2015**, *282*, 443 544–551. [CrossRef]
15. Gao, W.; Song, J.; Cao, H.; Lin, X.; Zhang, X.; Zheng, X.; Zhang, Y.; Sun, Z. Selective recovery of valuable metals from spent lithium-ion batteries—Process development and kinetics evaluation. *J. Clean. Prod.* **2018**, *178*, 833–845. [CrossRef]
16. He, L.P.; Sun, S.Y.; Mu, Y.Y.; Song, X.F.; Yu, J.G. Recovery of lithium, nickel, cobalt and manganese from spent lithium-ion batteries using L-tartaric acid as leachant. *ACS Sustain. Chem. Eng.* **2017**, *5*, 714–721. [CrossRef]
17. Yao, Y.; Zhu, M.; Zhao, Z.; Tong, B.; Fan, Y.; Hua, Z. Hydrometallurgical processes for recycling spent lithium-ion batteries: A critical review. *ACS Sustain. Chem. Eng.* **2018**, *6*, 13611–13627. [CrossRef]
18. Meshram, P.; Abhilash; Pandey, B.D.; Mankhand, T.R.; Deveci, H. Comparison of Different Reductants in Leaching of Spent Lithium Ion Batteries. *J. Met.* **2016**, *68*, 2613–2623. [CrossRef]
19. Bertuol, D.A.; Machado, C.M.; Silva, M.L.; Calgaro, C.O.; Dotto, G.L.; Tanabe, E.H. Recovery of cobalt from spent lithium-ion batteries using supercritical carbon dioxide extraction. *Waste Manage.* **2016**, *51*, 245–251. [CrossRef]
20. Zheng, Y.; Long, H.L.; Zhou, L.; Wu, Z.S.; Zhou, X.; You, L.; Yang, Y.; Liu, J.W. Leaching procedure and kinetic studies of cobalt in cathode materials from spent lithium ion batteries using organic citric acid as leachant. *Int. J. Environ. Res.* **2016**, *10*, 159–168. [CrossRef]
21. Fan, B.; Chen, X.; Zhou, T.; Zhang, J.; Xu, B. A sustainable process for the recovery of valuable metals from spent lithium-ion batteries. *Waste Manag. Res.* **2016**, *34*, 474–481. [CrossRef]
22. Santana, I.L.; Moreira, T.F.M.; Lelis, M.F.F.; Freitas, M.B.J.G. Photocatalytic properties of $Co_3O_4/LiCoO_2$ recycled from spent lithium-ion batteries using citric acid as leaching agent. *Mater. Chem. Phys.* **2017**, *190*, 38–44. [CrossRef]
23. Peng, C.; Hamuyuni, J.; Wilson, B.P.; Lundstrom, M. Selective reductive leaching of cobalt and lithium from industrially crushed waste Li-ion batteries in sulfuric acid system. *Waste Manag.* **2018**, *76*, 582–590. [CrossRef] [PubMed]
24. Nayaka, G.P.; Pai, K.V.; Manjanna, J.; Keny, S.J. Use of mild organic acid reagents to recover the Co and Li from spent Li-ion batteries. *Waste Manag.* **2016**, *51*, 234–238. [CrossRef] [PubMed]

25. Nayaka, G.P.; Zhang, Y.; Dong, P.; Wang, D.; Zhiu, Z.; Duan, J.; Li, X.; Lin, Y.; Meng, Q.; Pai, K.V.; et al. An environmental friendly attempt to recycle the spent Li-ion battery cathode through organic acid leaching. *J. Environ. Chem. Eng.* **2019**, *7*, 102854. [CrossRef]
26. Aaltonen, M.; Peng, C.; Wilson, B.P.; Lundstrom, M. Leaching of Metals from Spent Lithium-Ion Batteries. *Recycling* **2017**, *2*, 20. [CrossRef]
27. Nayaka, G.P.; Manjanna, J.; Pai, K.V.; Vadavi, R.; Keny, S.J.; Tripathi, V.S. Recovery of valuable metal ions form the spent lithium-ion battery using aqueous mixture of mild organic acid as alternative to mineral acids. *Hydrometallurgy* **2015**, *151*, 73–77. [CrossRef]
28. Nayaka, G.P.; Pai, K.V.; Santhosh, G.; Manjanna, J. Dissolution of cathode active material of spent Li-ion batteries using tartaric acid and ascorbic acid mixture to recover Co. *Hydrometallurgy* **2016**, *161*, 54–57. [CrossRef]
29. Dorella, G.; Mansur, M.B. A study of the separation of cobalt from spent Li-ion battery residues. *J. Power Sources* **2007**, *170*, 210–215. [CrossRef]
30. Nayl, A.A.; Elkhashab, R.A.; Badawy, S.M.; El-Khateeb, M.A. Acid leaching of mixed spent Li-ion batteries. *Arab. J. Chem.* **2017**, *10*, 3632–3693. [CrossRef]
31. Mantuano, D.P.; Dorella, G.; Elias, R.C.V.; Mansur, M.B. Analysis of a hydrometallurgical route to recover base metals from spent rechargeable batteries by liquid–liquid extraction with Cyanex 272. *J. Power Sources* **2006**, *159*, 1510–1518. [CrossRef]
32. Urbańska, W. Recovery of Co, Li, and Ni from Spent Li-Ion Batteries by the Inorganic and/or Organic Reducer Assisted Leaching Method. *Minerals* **2020**, *10*, 555. [CrossRef]
33. Heydarian, A.; Mousavi, S.M.; Vakilchap, F.; Baniasadi, M. Application of a mixed culture of adapted acidophilic bacteria in two-step bioleaching of spent lithium-ion laptop batteries. *J. Power Sources* **2018**, *378*, 19–30. [CrossRef]
34. Meshram, P.; Pandey, B.D.; Mankhand, T.R. Recovery of valuable metals from cathodic active material of spent lithium ion batteries: Leaching and kinetic aspects. *Waste Manag.* **2015**, *45*, 306–313. [CrossRef] [PubMed]
35. Lv, W.; Wang, Z.; Cao, H.; Zheng, X.; Jin, W.; Zhang, Y.; Sun, Z. A sustainable process for metal recycling from spent lithium-ion batteries using amonnium chloride. *Waste Manag.* **2018**, *79*, 545–553. [CrossRef] [PubMed]
36. Chen, X.; Guo, C.; Ma, H.; Li, J.; Zhou, T.; Cao, L.; Kang, D. Organic reductants based leaching: A sustainable process for the recovery of valuable metals from spent lithium ion batteries. *Waste Manag.* **2018**, *75*, 459–468. [CrossRef] [PubMed]
37. Pinto, P.S.; Lanza, G.D.; Ardisson, J.D.; Lago, R.M. Controlled Dehydration of $Fe(OH)_3$ to Fe_2O_3: Developing Mesopores with Complexing Iron Species for the Adsorption of β-Lactam Antibiotics. *J. Braz. Chem. Soc.* **2019**, *30*, 310–317. [CrossRef]
38. Xia, X.; Tu, J.; Zhang, Y.; Mai, Y.; Wang, X.; Gu, C.; Zhao, X. Freestanding Co_3O_4 nanowire array for high performance supercapacitors. *RSC Adv.* **2012**, *2*, 1835–1841. [CrossRef]
39. Allaedini, G.; Muhammad, A. Study of influential factors in synthesis and characterization of cobalt oxide nanoparticles. *J. Nanostructure Chem.* **2013**, *3*, 77. [CrossRef]
40. Wang, J.; He, Y.; Yang, Y.; Xie, W.; Ling, X. Research on quantifying the hydrophilicity of leached coals by ftir spectroscopy. *Physicochem. Probls. Miner. Process.* **2017**, *53*, 227–239. [CrossRef]
41. Tannenbaum, R.; Zubris, M.; David, K.; Ciprari, D.; Jacob, K.; Jasiuk, I.; Dan, N. FTIR Characterization of the Reactive Interface of Cobalt Oxide Nanoparticles Embedded in Polymeric Matrices. *J. Phys. Chem. B* **2006**, *110*, 2227–2232. [CrossRef]
42. Noriega, S.; Subramanian, A. Consequences of Neutralization on the Proliferation and Cytoskeletal Organization of Chondrocytes on Chitosan-Based Matrices. *Int. J. Carbohydr. Chem.* **2011**, 809743. [CrossRef]
43. Uznanski, P.; Zakrzewska, J.; Favier, F.; Kazmierski, S.; Bryszewska, E. Synthesis and characterization of silver nanoparticlesfrom (bis)alkylamine silver carboxylate precursors. *J. Nanopart. Res.* **2017**, *19*, 12. [CrossRef] [PubMed]
44. Funda, S.; Ohki, T.; Liu, Q.; Hossain, J.; Ishimaru, Y.; Ueno, K.; Shirai, H. Correlation between the fine structure of spin-coated PEDOT:PSS and the photovoltaic performance of organic/crystalline-silicon heterojunction solar cells. *J. Appl. Phys.* **2016**, *120*, 033103. [CrossRef]
45. Fila, D.; Hubicki, Z.; Kołodyńska, D. Recovery of metals from waste nickel-metal hydride batteries using multifunctional Diphonix resin. *Adsorption* **2019**, *25*, 367–382. [CrossRef]

46. Li, X.; Wang, Y.; Xie, X.; Huang, C.; Yang, S. Dehydration of fructose, sucrose and inulin to 5-hydroxymethylfurfural over yeast-derived carbonaceous microspheres at low temperatures. *RSC Adv.* **2019**, *9*, 9041–9048. [CrossRef]
47. Bounaas, M.; Bouguettoucha, A.; Chebli, D.; Reffas, A.; Harizi, I.; Rouabah, F.; Amrane, A. High efficiency of methylene blue removal using a novel low-cost acid treated forest wastes, Cupressus semperirens cones: Experimental results and modeling. *Particul. Sci. Technol.* **2019**, *37*, 504–513. [CrossRef]
48. Zhang, F.; Yuan, C.; Lu, X.; Zhang, L.; Zhang, X.; Che, Q. Facile growth of mesoporous Co_3O_4 nanowire arrays on Ni foam for high performance electrochemical capacitors. *J. Power Sources* **2012**, *203*, 250–256. [CrossRef]
49. Freitas, B.G.A.; Siqueira, J.M., Jr.; da Costa, L.M.; Ferreira, G.B.; Resende, J.A.L.C. Synthesis and Characterization of $LiCoO_2$ from Different Precursors by Sol-Gel Method. *J. Braz. Chem. Soc.* **2017**, *28*, 2254–2266. [CrossRef]
50. Lakshmanan, R.; Gangulibabu; Bhuvaneswari, D.; Kalaiselvi, N. Temperature Dependent Surface Morphology and Lithium Diffusion Kinetics of $LiCoO_2$ Cathode. *Met. Mater. Int.* **2012**, *18*, 249–255. [CrossRef]
51. Xie, J.; Cao, H.; Jiang, H.; Chen, Y.; Shi, W.; Zheng, H.; Huang, Y. Co_3O_4-reduced graphene oxide nanocomposite as an effective peroxidase mimetic and its application in visual biosensing of glucose. *Anal. Chim. Acta* **2013**, *796*, 92–100. [CrossRef]
52. Qi, C.; Koenig, G.M. High-Performance $LiCoO_2$ Sub-Micrometer Materials from Scalable Microparticle Template Processing. *ChemistrySelect* **2016**, *1*, 3992–3999. [CrossRef]
53. Santiago, E.I.; Andrade, A.V.C.; Paiva-Santos, C.O.; Bulhoes, L.O.S. Structural and electrochemical properties of $LiCoO_2$ prepared by combustion synthesis. *Solid State Ion.* **2003**, *158*, 91–102. [CrossRef]
54. Zeng, X.; Li, J.; Shen, B. Novel approach to recover cobalt and lithium from spent lithium-ion battery using oxalic acid. *J. Hazard. Mater.* **2015**, *295*, 112–118. [CrossRef] [PubMed]
55. Jha, A.K.; Jha, M.K.; Kumari, A.; Sahu, S.K.; Kumar, V.; Pandey, B.D. Selective separation and recovery of cobalt from leach liquor of discarded Li-ion batteries using thiophosphinic extractant. *Sep. Purif. Technol.* **2013**, *104*, 160–166. [CrossRef]
56. Zhang, L.; Zhang, K.; Shi, Z.; Zhang, S. LiF as an Artificial SEI Layer to Enhance the High-Temperature Cycle Performance of $Li_4Ti_5O_{12}$. *Langmuir* **2017**, *33*, 11164–11169. [CrossRef]
57. Babkair, S.S.; Azam, A. Color Centers Formation in Lithium Fluoride Nanocubes Doped with Different Elements. *J. Nanomater.* **2013**, *872074*, 1–8. [CrossRef]
58. Yu, X.Q.; Sun, J.P.; Tang, K.; Li, H.; Huang, X.J.; Dupont, L.; Maier, J. Reversible lithium storage in LiF/Ti nanocomposites. *Phys. Chem. Chem. Phys.* **2009**, *11*, 9497–9503. [CrossRef]
59. Ungár, T.; Gubicza, J.; Ribárik, G.; Pantea, C.; Zerda, T.W. Microstructure of carbon blacks determined by X-ray diffraction profile analysis. *Carbon* **2002**, *40*, 929–937. [CrossRef]
60. Tao, S.; Zhan, Z.; Wang, P.; Meng, G. Chemical stability study of Li_2SO_4 on the operation condition of a H_2/O_2 fuel cell. *Solid State Ion.* **1999**, *116*, 29–33. [CrossRef]
61. Kohl, M.; Bruckner, J.; Bauer, I.; Althues, H.; Kaskel, S. Synthesis of highly electrochemically active Li_2S nanoparticles for Lithium-sulfur-Batteries. *J. Mater. Chem. A* **2015**, *3*, 16307–16312. [CrossRef]
62. Pan, A.; Wang, Y.; Xu, W.; Nie, Z.; Liang, S.; Nie, Z.; Wang, C.; Cao, G.; Zhang, J. High-performance anode based on porous Co_3O_4 nanodiscs. *J. Power Sources* **2014**, *255*, 125–129. [CrossRef]
63. Lu, Y.; Wang, J.; Zeng, S.; Zhou, L.; Xu, W.; Zheng, D.; Liu, J.; Zeng, Y.; Lu, X. An ultrathin defect-rich Co_3O_4 nanosheet cathode for high-energy and durable aqueous zinc ion batteries. *J. Mater. Chem. A* **2019**, *7*, 21678–21683. [CrossRef]
64. Rahman, M.M.; Wang, J.Z.; Deng, X.L.; Li, Y.; Liu, H.K. Hydrothermal synthesis of nanostructured Co_3O_4 materials under pulsed magnetic field and with an aging technique, and their electrochemical performance as anode for lithium-ion battery. *Electrochim. Acta* **2009**, *55*, 504–510. [CrossRef]
65. Zhou, H.; Lv, B.; Wu, D.; Xu, Y. Synthesis of the polycrystalline Co3O4 nanowires with excellent ammonium perchrolate catalytic decomposition property. *Mater. Res. Bull.* **2014**, *60*, 492–497. [CrossRef]